Dynamic Synchrophasor Estimation by Extended Kalman Filter

Roberto Ferrero, *Senior Member, IEEE*, Paolo Attilio Pegoraro, *Senior Member, IEEE*, Sergio Toscani, *Senior Member, IEEE*

***Abstract*—Fast synchronized measurements of phasor, frequency and rate of change of frequency are expected to be very important for the automated control actions in the smart grid context. In this regard, measurement latency must be kept as short as possible for an effective control implementation when networks characterized by extremely fast dynamics are concerned. Kalman filter based estimation algorithms appear to be attractive in this context, however the conventional implementations suffer from significant limitations in their ability to deal with different types of dynamic conditions, due to approximations in the model and in the associated uncertainty. This paper proposes an innovative solution, based on an extended Kalman filter algorithm using a Taylor model, which is shown to provide improved tracking ability in a vast range of dynamic conditions. A novel element in the proposed technique is the representation of model uncertainty, which takes into account the intrinsic correlation among errors that appear in the state-space description under dynamic conditions. A compatibility check between the forecast and measurement result is also introduced as an effective and metrologically-sound approach to detect large unexpected changes in the tracked parameters, in order to achieve a fast response of the algorithm also in those conditions. The algorithm performance is thoroughly investigated by means of simulation, to demonstrate the significant improvement compared to other Kalman-filter solutions in some conditions of practical relevance.**

***Index Terms*—Phasor measurement units, Frequency estimation, Kalman filters, Correlation, Power system harmonics, Power system measurements, Voltage measurement, Measurement uncertainty**

I. Introduction

Synchronized measurements of electrical signals represent the emerging technology that plays the leading role in the modernization of power network monitoring. Thanks to a universal time coordinated (UTC) reference, e.g. from Global Positioning System receivers, each measurement is associated with a time instant and thus timestamped with submicrosecond accuracy before being sent to concentrators and control centers [1].

The concept of synchronized measurements has been applied to ac transmission networks for at least ten years. The most noticeable practical application is represented by phasor measurement units (PMUs) [2] providing estimates of the phasor, frequency and rate of change of frequency (ROCOF) of the monitored electrical signals at high reporting rates (reporting intervals in the order of tens of milliseconds are achievable). This feature enables a much more accurate supervision of the power system as well as the employment of advanced grid protection control and automation techniques based on wide area monitoring which were completely unfeasible otherwise; work is ongoing for their implementation.

The increasing interest of the transmission system operators (TSOs), of the manufacturers and of the scientific community towards such powerful instruments triggered a standardization process. PMU functionalities and cabalilities are ruled by standard IEC-IEEE 60255-118-1 [3] and its forerunners IEEE C37.118.1-2011 [4] and IEEE C37.118.1a-2014 [5]. The concept of "dynamic synchrophasor" is introduced: PMU measurements should comply with accuracy requirements with either steady state or dyanmic input signals (for example containing amplitude or phase modulation, frequency ramp, etc...) defined by the standards. The underlying idea is that these test signals are designed to stress the measurement capability of the PMUs while, at the same time, resembling the possible operating scenarios that are faced during typical operation.

In the smart grid (SG) context, automated control actions based on accurate and timely measurements are expected to become disruptive tools also in distribution networks. However it should be noticed that the challenges to be faced are completely different. One of them is measurement latency, which is key for an effective control of grids characterized by extremely fast dynamics, because of the huge penetration of devices based on power electronics.

From a broader perspective, measurement algorithms play a fundamental role in synchronized measurements [1], particularly under dynamic conditions. For these reasons, different proposals have been presented in the literature concerning dynamic synchrophasors, frequency and ROCOF measurements. Each one is characterized by its own advantages and drawbacks that make it particularly suited to fulfil a specific application.

In [6], Taylor-Fourier (TF) filters are introduced and employed for synchrophasor, frequency and ROCOF estimations. Filter coefficients are obtained starting from a Taylor expansion of the synchrophasor around the reporting instant while inverting the problem in a least squares sense. The same model is used in [7], [8] to correct discrete fourier transform (DFT)

Dr. Pegoraro's work was partially funded by Fondazione di Sardegna for the research project "SUM2GRIDS, Solutions by mUltidisciplinary approach for intelligent Monitoring and Management of power distribution GRIDS".

R. Ferrero is with the Department of Electrical Engineering and Electronics, University of Liverpool, Liverpool, UK (e-mail: roberto.ferrero@liverpool.ac.uk).

P. A. Pegoraro is with the Department of Electrical and Electronic Engineering of the University of Cagliari, Piazza d'Armi, 09123 Cagliari, Italy (e-mail: paolo.pegoraro@unica.it).

S. Toscani is with Dipartimento di Elettronica, Informazione e Bioingegneria, Politecnico di Milano, Milan, Italy (e-mail: sergio.toscani@polimi.it).

measurements of the fundamental phasor. In [9], the model is exploited to develop a two-channel algorithm that allows simultaneous compliance with both P and M performance classes defined in [3], by selecting the best estimate according to input conditions. In [10], TF model is extended in order to include harmonics, while in [11] the same model is adaptively expanded with a frequency support which is refreshed by means of compressive sensing techniques.

From another perspective, [12] computes the Space Vector (SV) signal starting from the three phase samples while using low pass filtering and truncated Taylor expansions of its magnitude and phase in order to measure positive sequence synchrophasor and frequency. The idea of exploiting the peculiar characteristics of three-phase systems together with a TF model of the SV signal is proposed in [13].

When considering some control applications, fast response and low latency are mandatory requirements. In this case, one viable solution is using a Taylor expansion of the phasor in order to define a suitable Kalman filter (KF). With this approach, the classical DFT-like model [14] commonly used for the KF can be extended to track phasor variations thus resulting in the so-called Taylor-Kalman filter (TKF) [15]. In [16] TKF is enhanced in terms of phasor derivatives and phase angle dynamics. In [17] a smoothed TKF allowing remarkable accuracy under off-nominal frequency conditions is presented. The aforementioned KF formulations consider the fundamental frequency component only, but harmonics can be present in the input signal, thus jeopardizing synchrophasor and frequency measurements. In order to overcome this issue the model can be modified to include also harmonics as proposed in [18] and in [19]; this enhanced version of TKF also allows extracting harmonic synchrophasors.

Regardless of the selected KF implementation, all the above mentioned proposals are based on a Taylor expansion of the phasor, namely a complex quantity, around the measurement instant. This permits a linearization of the model, but it reqires considering complex derivatives, which do not allow separate modeling of amplitude and phase angle dynamics. In [20] a new approach, namely the Taylor Extended Kalman filter (TEKF) is introduced: amplitude and phase angle derivatives appears as state variables in this case. It should be noticed that frequency is also a state variable being proportional to the phase angle derivative. Harmonics are included and constrained to have frequencies that are integer multiples of the fundamental phasor frequency.

In this paper, the TEKF approach is extended and revisited from a measurement viewpoint. The performance of the TEKF is strongly related to how well the statistic behavior of measurement and model errors is represented by the covariance matrices employed in the implementation. Estimating the values of those matrices is certainly not an easy task, but the problem is even more complex. The optimal Kalman gain is computed supposing that the model error in each time instant is an independent realization of a zero-mean random vector from a multivariate gaussian distribution. Of course, this assumption is not met if this error is due to an underparametrization of the dynamic model, as it occurs in practice: this unavoidably results in time correlation of the model error.

In this paper an innovative technique is proposed to solve this limitation of conventional Kalman filters. The more realistic representation of the model error immediately turns in improved estimates. The new model is particularly effective in representing higher order dynamics, and for this reason benefits are clearly visible in ROCOF measurements.

II. Synchrophasor Measurement and Kalman Filter Model

In general, implementing a KF-based algorithm allowing synchrophasor, frequency and ROCOF estimations from the time domain signal samples requires defining:

1) a set of state variables which are somehow related to the quantities to be measured (synchrophasor, frequency and ROCOF);
2) a dynamic model that describes the time evolution of the state variables;
3) an algebraic equation mapping the states to the acquired samples of the waveform;
4) an algebraic equation linking state variables to the quantities to be measured.

We start by assuming an expression of the measured signal:

$$\begin{aligned} s(t) &= a_1(t)\cos\left[\omega_0 t + \varphi_1(t)\right] \\ &+ \sum_{h=2}^{M} a_h(t)\cos\left[h\omega_0 t + \varphi_h(t)\right] \end{aligned} \tag{1}$$

where ω_0 is the rated angular speed (corresponding to the rated frequency $f_0 = \omega_0/2\pi$), $a_h(t)$ and $\varphi_h(t)$, with $h = 1, \ldots, M$ are the amplitude and phase angle of the hth order harmonic component ($h = 1$ corresponds to the fundamental term). Magnitude and phase angle are time-varying functions (which allows considering also off-nominal frequency) assumed to be slowly changing over a fundamental period.

Synchrophasors are defined as the phasors referred to specific and universally defined time instants (belonging to an UTC timescale for instance) considering a reference frame that rotates at the rated angular speed ω_0. From (1), the expression of the fundamental synchrophasor is obtained straightforwardly:

$$p\left(t\right) = a_1\left(t\right) e^{j\varphi_1(t)} \tag{2}$$

Frequency and ROCOF results from the first and second order derivatives of the fundamental phase angle as follows:

$$f_1\left(t\right) = \frac{\omega_1(t)}{2\pi} = f_0 + \frac{1}{2\pi}\frac{d\varphi_1\left(t\right)}{dt} \tag{3}$$

$$\text{ROCOF}\left(t\right) = \frac{df_1(t)}{dt} = \frac{1}{2\pi}\frac{d^2\varphi_1(t)}{dt^2} \tag{4}$$

(1) can be rewritten in a more convenient way for KF implementation:

$$s\left(t\right) = \Re\left[\sum_{h=1}^{M} a_h\left(t\right) e^{j\psi_h(t)}\right] = \sum_{h=1}^{M} a_h\left(t\right)\cos\left[\psi_h\left(t\right)\right] \tag{5}$$

Here the phase-angle function $\psi_1(t)$ has been introduced, which is the cosine argument of the fundamental term thus adding up the contribution of the time varying phase angle

φ_1 and that of the roatating reference frame. Therefore it represents the fundamental phase angle when measured in a stationary reference frame. In general, $\psi_h(t) = h\omega_0 t + \varphi_h(t)$.

Now, according to point 1 and 2 of the above list, a set of state variables and a model representing the time evolution of the harmonic synchrophasors appearing in the output equation (5) are required. For this purpose, let us consider the following set of state variables (time dependency is dropped hereafter for the sake of brevity):

1) fundamental angular frequency ω_1 along with its derivatives $\omega_1^{(k)}$ up to order N_{ω_1}, grouped in the state subvector $\mathbf{x}_{\omega_1}$ (symbol $'\top'$ denotes the transpose operator):
$$\mathbf{x}_{\omega_1} = \begin{bmatrix} \omega_1 & \omega_1^{(1)} & \cdots & \omega_1^{(N_\omega)} \end{bmatrix}^\top \tag{6}$$
2) fundamental synchrophasor amplitude along with its derivatives $a_1^{(k)}$ up to order N_1.
3) fundamental phase angle ψ_1 with respect to the stationary reference frame. This variable together with those related to the fundamental amplitude are included in subvector $\mathbf{x}_1$:
$$\mathbf{x}_1 = \begin{bmatrix} a_1 & a_1^{(1)} & \cdots & a_1^{(N_1)} & \psi_1 \end{bmatrix}^\top \tag{7}$$
4) hth order harmonic synchrophasor amplitude a_h
5) hth order harmonic phase angle ψ_h in the stationary reference frame. Subvector $\mathbf{x}_h$ is thus defined as follows:
$$\mathbf{x}_h = \begin{bmatrix} a_h & \psi_h \end{bmatrix}^\top \tag{8}$$

The state vector can be thus defined by concatenating the previously introduced subvectors:

$$\mathbf{x} = \begin{bmatrix} \mathbf{x}_{\omega_1}^\top & \mathbf{x}_1^\top & \mathbf{x}_2^\top & \cdots & \mathbf{x}_M^\top \end{bmatrix}^\top \tag{9}$$

the state-space size is therefore $N = N_{\omega_1} + N_1 + 2M + 3$.

The dynamic model employed in the KF should describe the time evolution of the state vector (9); in this work such time evolution is assumed to be expressed by a truncated Taylor expansion around each instant. If the derivatives of ω_1 having orders greater than N_{ω_1}, the derivatives of the fundamental amplitude above order N_1 and all the harmonics' amplitudes derivatives were zero, the following state-space expression would exactly describe the dynamics:

$$\frac{d\mathbf{x}}{dt} = \mathbf{A}_c \mathbf{x} \tag{10}$$

where:

$$\mathbf{A}_c = \begin{bmatrix} \mathbf{A}_{c,\omega_1} & \mathbf{0} & \mathbf{0} & \cdots & \mathbf{0} \\ \mathbf{A}_{c,1,\omega_1} & \mathbf{A}_{c,1} & \mathbf{0} & \cdots & \mathbf{0} \\ \mathbf{A}_{c,2,\omega_1} & \mathbf{0} & \mathbf{0} & \cdots & \mathbf{0} \\ \vdots & \vdots & \vdots & \ddots & \mathbf{0} \\ \mathbf{A}_{c,M,\omega_1} & \mathbf{0} & \mathbf{0} & \cdots & \mathbf{0} \end{bmatrix} \tag{11}$$

submatrix $\mathbf{A}_{c,\omega_1}$ is a $(N_{\omega_1}+1) \times (N_{\omega_1}+1)$ upper shift matrix while $\mathbf{A}_{c,1}$ is a $(N_1+2) \times (N_1+2)$ upper shift matrix whose element in position (N_1+1, N_1+2) is set to zero. Matrix $\mathbf{A}_{c,1,\omega_1} \in \mathbb{R}^{(N_1+2)\times(N_{\omega_1}+1)}$ has the following structure:

$$\mathbf{A}_{c,1,\omega_1} = \begin{bmatrix} \mathbf{0}_{(N_1+1)\times 1} & \mathbf{0}_{(N_1+1)\times N_\omega} \\ 1 & \mathbf{0}_{1\times N_\omega} \end{bmatrix} \tag{12}$$

since the phase angle derivative is the angular speed. Similarly, focusing on harmonics:

$$\mathbf{A}_{c,h,\omega_1} = \begin{bmatrix} 0 & 0 \\ h & 0 \end{bmatrix} \tag{13}$$

because the phase of the harmonics rotates at an angular speed that is h times the fundamental one. The adopted model assumes that the evolutions of the harmonic phases are driven by the system frequency. Since harmonics have much smaller magnitudes with respect to the fundamental, there is no need for a more detailed description of their dynamics as far as fundamental synchrophasor measurement is concerned.

Measurement equations can be easily derived from the signal representation in (5) and the state variables defined in (6)-(9). The following nonlinear, time-varying equation holds true:

$$\begin{aligned} s(t) = c(\mathbf{x}, t) = x_{N_\omega+2} \cos\left(x_{N_\omega+N_1+3}\right) \\ + \sum_{h=2}^{M} x_{N_\omega+N_1+2h} \cos\left(x_{N_\omega+N_1+2h+1}\right) \end{aligned} \tag{14}$$

where x_i stands for the ith element of the state vector.

For practical implementations we have to move to the discrete time domain in order to deal with sampled signals, being T_s the sampling interval. While the discrete-time representation of (14) can be directly obtained by sampling, the state-space equation has to be discretized as (only the time index n is reported):

$$\mathbf{x}(n+1) = \mathbf{A}\mathbf{x}(n) = e^{\mathbf{A}_c T_s}\mathbf{x}(n) \tag{15}$$

As an example, submatrix $\mathbf{A}_{\omega_1}$of $\mathbf{A}$ (describing frequency dynamics) becomes:

$$\mathbf{A}_{\omega_1} = \begin{bmatrix} 1 & T_s & \cdots & \frac{T_s^{N_{\omega_1}}}{N_{\omega_1}!} \\ 0 & 1 & \ddots & \vdots \\ 0 & 0 & \ddots & T_s \\ 0 & 0 & \cdots & 1 \end{bmatrix} \tag{16}$$

and similarly for the other blocks of $\mathbf{A}_h$ which define the amplitude updates. The phase angle evolutions of the fundamental and harmonics are instead described by the simple equation $\psi_h(n+1) = \psi_h(n) + h\omega_1(n)T_s$.

The continous-time equations in (10) and, as a consequence, their discrete-time counterparts in (15), are the results of an approximation since the dynamic Taylor series for each quantity has been truncated to a predetermined order. Thus a process model $\mathbf{w}_c$ must be considered in (10), in order to take into account the model error introduced by such approximation. In the discrete time equation, the zero-mean process noise $\mathbf{w}(n)$ is analogously considered and parametrized by the associated covariance matrix $\mathbf{Q}$. In Section III, a detailed discussion about process uncertainty modeling is reported.

Once all the equations have been defined, it is possible to use them in the extended Kalman filter estimation steps (TEKF algorithm):

1) *Forecast step*. The state forecast at time $(n+1)T_s$ is obtained from the previously estimated state $\mathbf{x}(n)$ (along

with its covariance matrix $\mathbf{P}(n)$) by using the following equations:

$$\mathbf{x}^F(n+1) = \mathbf{A}\mathbf{x}(n) \tag{17}$$

$$\begin{aligned}\mathbf{P}^F(n+1) &= \mathbf{A}\mathbf{P}(n)\mathbf{A}^\top + \mathbf{Q} \\ &= \begin{bmatrix}\mathbf{A} & \mathbf{I}\end{bmatrix}\begin{bmatrix}\mathbf{P}(n) & \mathbf{0} \\ \mathbf{0}^\top & \mathbf{Q}\end{bmatrix}\begin{bmatrix}\mathbf{A} & \mathbf{I}\end{bmatrix}^\top\end{aligned} \tag{18}$$

where superscript ^{F} denotes forecast quantities while $\mathbf{Q}$ is the aforementioned covariance matrix defining process noise. The second line in (18) explicitly shows how the covariance matrix of the forecast is computed by considering previous estimates and process noise as uncorrelated. This assumption will be discussed and removed in Section IV.

2) *Assimilation step*. The previously obtained state forecast $\mathbf{x}^F(n+1)$ is then refined by using the new sample $s(n+1) \triangleq s(t)|_{t=(n+1)T_s}$. Assuming that samples are corrupted by zero mean noise characterized by known variance R, the unbiased state estimate having minimum covariance matrix results:

$$\begin{aligned}\mathbf{x}(n+1) &= \mathbf{x}^F(n+1) \\ &+ \mathbf{K}(n+1)[s(n+1) - c(\mathbf{x}^F(n+1), (n+1)T_s)]\end{aligned} \tag{19}$$

where the Kalman matrix gain $\mathbf{K}(n+1)$ is obtained by computing:

$$\begin{aligned}\mathbf{K}(n+1) &= \mathbf{P}^F(n+1)\mathbf{C}^\top(n+1) \\ &\cdot [\mathbf{C}(n+1)\mathbf{P}^F(n+1)\mathbf{C}^\top(n+1) + R]^{-1}\end{aligned} \tag{20}$$

with

$$\mathbf{C}(n+1) = \left.\frac{dc(\mathbf{x},t)}{d\mathbf{x}^\top}\right|_{\substack{\mathbf{x}=\mathbf{x}^F(n+1) \\ t=(n+1)T_s}} \tag{21}$$

Equation (19) is a weighted average between the state estimates coming from forecast and measurement, where their weights are represented by the inverses of the corresponding covariance matrices. The covariance matrix of the optimal state estimation is easily obtained as:

$$\mathbf{P}(n+1) = (\mathbf{I} - \mathbf{K}(n+1)\mathbf{C}(n+1))\mathbf{P}^F(n+1) \tag{22}$$

The TEKF directly uses the information about frequency dynamics since it links all the harmonic phase-angle evolutions to the fundamental frequency while it describes frequency changes by using a truncated Taylor expansion around the measurement time. Different Taylor expansion orders can be adopted for fundamental amplitude and phase angle, thus allowing a tailored model for both amplitude and phase variations.

Since frequency and ROCOF have to be estimated, N_{ω_1} must be at least equal to one, otherwise ROCOF cannot be measured. However, a better choice is $N_{\omega_1} \geq 2$, which allows including ROCOF dynamics in the model, as it will be discussed in more detail during the next section.

III. Uncertainties and Issues of the Kalman Filter Approach

A. Model and Measurement Uncertainties

KF-based estimation procedure requires defining the covariance matrix (uncertainties) summarizing the statistical properties of the model errors due to the approximation introduced in (15) and the variance of the error affecting acquired samples. Once the uncertainty framework is defined, achieved performances depend on how much the assumptions employed in formulating the KF reflect actual working conditions.

In order to define the covariance matrix $\mathbf{Q}$, a possible approach starts from assumptions about the possible dynamics that the electric signals may undergo. For this purpose, the signals suggested in the synchrophasor standards [3], [4] to test compliance under dynamic conditions are considered. Signals and test conditions reported in [3] refer to PMUs having currents or voltages as inputs: for this reason, the analysis in the following is general. Typically, in practical implementations, frequency measurements are computed from voltages, but the algorithms proposed in this paper apply to any single-phase signal. In this respect, it is interesting to notice that the state definition in (9) and the corresponding models including harmonics well suit also current synchrophasor measurements, where harmonic content might be higher.

When phasor amplitude dynamics is taken into account, the most significant test signals are those containing amplitude modulation (AM). In these tests, the amplitude of the synchrophasor can be decomposed into a constant term superimposed to a sinusoidal one as follows:

$$a(t) = X_m(1 + k_x \cos(2\pi f_m t)) \tag{23}$$

where f_m is the modulation frequency while k_x represents modulation depth; X_m is the peak amplitude without modulation. When a N_1th order expansion of the amplitude is considered in the dynamic model, the N_1+1 order derivative is implicitly assumed to be zero; thus, the model error arising from this constraint must be considered. The maximum value of the derivative N_1+1 under AM is thus used to define the standard deviation of the corresponding model error. In particular, from (23), when a second order expansion is adopted, a model error arises since the third derivative $a^{(3)}$ has been neglected. Its maximum value can be easily obtained by differentiation as follows ($X_m = 1$ is supposed):

$$\max_t\{a^{(3)}(t)\} = k_x\omega_m^3 \tag{24}$$

where $\omega_m = 2\pi f_m$. Supposing that the sampling rate is very high with respect to the modulation frequency, the neglected derivative can be considered as constant during each sampling interval. Under this assumption we obtain a maximum model amplitude error equal to $k_x\omega_m^3 T_s$, which can be divided by a proper factor c (depending on the assumed probability distribution and confidence level) and then squared in order to get the variance of the error to be included in $\mathbf{Q}$. It is important to notice that error is due an incomplete dynamic model, thus in general it cannot be considered as a white process. Once the error on the highest-order derivative is defined, those corresponding to the other derivatives can be

obtained by means of integration and thus $\mathbf{Q}$ is filled with the variances of all the magnitude derivatives. Off-diagonal elements (covariances) are obtained by supposing unitary correlation.

When we focus on phase angle dynamics, similar considerations apply. In this case, the fastest variations that can be expected are those related to the cosinusoidal phase-angle modulation (PM) as suggested by [3], [4]. For a phase angle expansion order $N_{\psi_1} = N_{\omega_1} + 1$ we obtain:

$$\begin{aligned} \delta_{N_{\psi_1},1} &= k_a \omega_m^{N_{\psi_1}} T_s \\ &\vdots \\ \delta_{0,1} &= k_a \omega_m^{N_{\psi_1}} \frac{T_s^{N_{\psi_1}}}{N_{\psi_1}!} \end{aligned} \tag{25}$$

where k_a is the modulation parameter, ω_m has the same meaning as before, and $\delta_{k,1}$ is the maximum error in the state-space equation relating to the kth phase derivative of the fundamental component. Variances and covariances can be obtained from maximum errors as previously described.

It is interesting to notice that other dynamic conditions, such frequency ramp, would be perfectly matched by a second order model, without the need for higher degree derivatives. As for the harmonics, we have two state variables for each order h in the model: its magnitude and phase angle. Magnitude is considered as constant in the model, thus it is possible to use the maximum expected variation of the harmonic magnitude during T_s (divided by a proper factor) to fill the corresponding term in $\mathbf{Q}$. The phase-angle of each harmonic is instead strictly tied to the dynamics of the fundamental phase angle. The derivative of the hth order harmonic phase angle is thus assumed to be equal to the derivative of the fundamental phase multiplied by h. This results in perfect correlation between the derivatives at harmonic and fundamental frequencies, therefore the model error for the phase angle of each harmonic can be derived by scaling the corresponding error of the fundamental. For the same reason, perfect correlation is also assumed among all model errors related to harmonic phase angles.

The variance of the measured samples can be chosen by considering two different sources of uncertainty: the foreseen level of error in the measurement process and the level of unmodeled disturbances that can affect the samples. The latter contribution reflects the components that are not included in the model and thus in the state space.

In the next section, the limits of the presented error model are discussed with examples and the ground for the generalization proposed in Section IV is prepared.

B. Issues Under Dynamic Conditions

The previously introduced TEKF has been implemented and tested under the following assumptions:

- $f_0 = 50\,\text{Hz}$ rated frequency.
- Modulation frequencies f_m up to $5\,\text{Hz}$ have been considered; the maximum value has been used to obtain covariance matrix $\mathbf{Q}$.
- Modulation parameters up to k_x and k_a up to 0.1 have been taken into account; covariance matrix $\mathbf{Q}$ has been obtained from the maximum values.

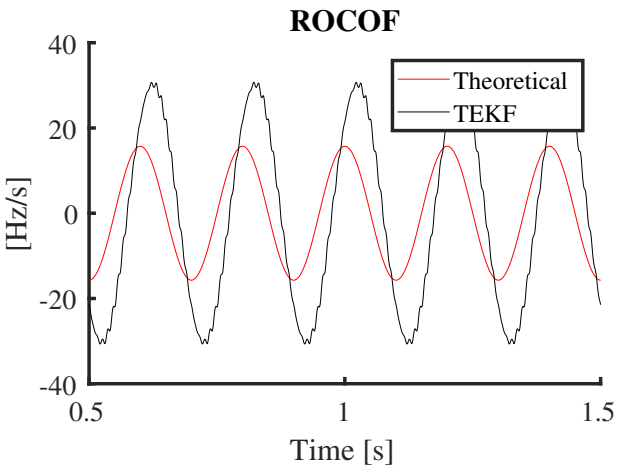

Fig. 1. TEKF ROCOF measurements in case of phase modulation test.

- Maximum variation of the harmonic magnitudes within a sampling interval is supposed to be 10^{-4} p.u. in order to compute the remaining elements of $\mathbf{Q}$.
- Signal amplitude is assumed to be equal to $1\,$p.u. for steady-state amplitude tests; $X_m = 1\,$p.u. is considered for AM tests.
- The standard deviation of the measurements is considered to be $0.01\,$p.u. (thus corresponding to $R = 10^{-4}$) hence $40\,$dB signal to noise ratio.

Test results under dynamic condition reveal some issues. For example, Fig. 1 reports the obtained ROCOF estimates under $5\,$Hz PM with $k_a = 0.1$. The graphs reveals that measured ROCOF is clearly delayed, and this is mainly due to errors in the dynamic model employed for KF implementation.

As described above, the process noise is intrisically considered as white (thus no correlation between two consecutive sampling intervals) and this description corresponds to a random walk model for the derivative $N_{\psi_1} + 1$ of the phase angle. Under PM conditions, the phase angle (without the rotating contribution) of the fundamental component is instead sinusoidal and its derivatives thus follow the same trend in phase or quadrature. Every correction of ROCOF estimation is slowed down by the wrong assumption about the random behavior of the model error and thus measured samples take longer in driving the estimates towards the correct trend. Section IV discusses a proposal to deal with this issue.

IV. Proposed Generalization of the Kalman Filter

The conventional implementation of the TEKF algorithm was summarized in Sec. II. In particular, (18) describes the state uncertainty of the forecast step, due to the uncertainty propagation through the dynamic model and the addition of the model uncertainty. The validity of (18) relies on the assumption that those two contributions are independent of each other, which is justified in the conventional formulation of the Kalman Filter because the model uncertainty is decribed in terms of white noise added to the dynamic model equations. As discussed in Sec. III, however, this assumption is not true in the considered application, because the model uncertainty

mainly takes into account the un-modeled dynamics of the state, i.e., the higher-order derivatives of the state variables, which do not behave like white noise. In fact, since during regular operation the dynamics of power system signals are typically rather slow with respect to the sampling rate (see, e.g., real signals in [18] and [21]), there might be a strong correlation between model errors affecting two consecutive samples. For this reason, in the considered application a correlation coefficient equal to 1 has been assumed for errors due the un-modeled higher-order derivatives of amplitude and phase of the fundamental component. Zero correlation has been considered for the other variables associated with the harmonics, to avoid model constraints that cannot be justified from *a priori* assumptions on their dynamics.

The correlation between two consecutive samples of the equivalent noise modeled by $\mathbf{Q}$ produces a correlation between the two contributions to the forecast state uncertainty $\mathbf{P}^F(n+1)$ in (18), because $\mathbf{P}(n)$ depends on $\mathbf{Q}$ from the previous iteration. This can be considered by introducing nonzero off-diagonal blocks in the block diagonal matrix appearing in (18), which therefore becomes:

$$\mathbf{P}^F(n+1) = \begin{bmatrix}\mathbf{A} & \mathbf{I}\end{bmatrix} \begin{bmatrix}\mathbf{P}(n) & \mathbf{S}(n) \\ \mathbf{S}(n)^\top & \mathbf{Q}\end{bmatrix} \begin{bmatrix}\mathbf{A} & \mathbf{I}\end{bmatrix}^\top \qquad (26)$$

where $\mathbf{I}$ is the identity matrix and $\mathbf{S}$ is a matrix that allows considering correlation between errors affecting the state evolution predicted by the model and the previously estimated state. Neglecting such a correlation may produce a significant under-estimation of the uncertainty $\mathbf{P}^F(n+1)$ of the forecast state, which in turn is reflected into a wrong assimilation step, due to excessively relying on the model forecast with respect to the measurement result. This explains the issues reported in Sec. III and shown in Fig. 1.

It should be noted that neither $\mathbf{S}$ nor the correlation coefficients in it are constant over time, as the correlation depends on the relative weight between the forecast uncertainty and the measurement uncertainty, where the former changes over time. Initially, the forecast uncertainty will be very high and the assimilation step will mainly rely on the measurement; therefore, the correlation will be negligible. As the TEKF algorithm converges, the forecast uncertainty will decrease and the correlation will increase, up to a maximum value reached when the algorithm is in steady-state conditions.

The correlation coefficients in $\mathbf{S}$ can be calculated through Monte Carlo simulations. Strictly speaking, they should be calculated for each iteration of the algorithm, but this would imply a huge computational burden and would be absolutely unfeasible in real-time applications. The solution proposed in this paper is to use constant correlation coefficients, calculated offline based on the expected uncertainties of the state and the measurement when the TEKF algorithm reaches a steady state. With this approach, the real-time computational burden is only slightly increased compared to the original TEKF, and it remains acceptable for the considered application.

The main drawback of this approach is that the constant correlation coefficients would represent a large overestimate of the actual correlation during large transients, e.g. step changes in the measured signals, before the algorithm goes back to a steady state. To avoid affecting the algorithm performance during those transients, the correlation is proposed to be introduced into the algorithm only when the iterations get close to convergence, and removed during the transients.

The presence of large transients can be effectively detected by checking the compatibility between the forecast and the measurement at each iteration. Indeed, from a measurement point of view, the assimilation step in the Kalman Filter consists in merging two independent estimates of the same quantities (one obtained from the model and one from the measurement). This operation is meaningful only if the two estimates are compatible (at a rather conservative confidence level: here a coverage factor equal to 5 have been used). With an appropriate modelling of the uncertainty sources, the two estimates are expected to be compatible most of the time; if they become incompatible at any iteration, it means that an unexpected large change in the signal has occurred. This also means that the forecast uncertainty has been under-estimated, and using it in the assimilation step would lead to wrong results.

The proposed solution is to re-initialize the state forecast uncertainty to large values and set all correlation coefficients to zero, when a large transient is detected, and re-introduce the correlation when the forecast uncertainty falls below a pre-defined threshold again, meaning that the algorithm is converging again.

V. Tests and Results

The method proposed in Section IV has been implementend and tested with the same assumptions and test signals as in Section III-B. Correlation matrix $\mathbf{S}$ have been pre-computed with preliminary Monte-Carlo iterations by considering a PM input signal. For each test condition, results are reported in terms of Total Vector Error (TVE), frequency error (FE or its absolute value |FE|) and ROCOF error (RFE or its absolute value |RFE|). Performance achieved by the proposed approach (TEKF-corr) have been compared to those obtained with conventional TEKF.

A. Modulation Tests

AM and PM tests are devoted at stressing the dynamic tracking capability of the presented method. First of all the results of PM tests (5 Hz modulation frequency, $k_a = 0.1$) are shown in order to check how the proposed method is able to deal with the issues discussed in Section III-B. In particular, Fig. 2 reports the estimated ROCOF when correlation is included in the model, as discussed in Section IV, on the same time window of the PM test as before[1]. The filter is able to follow second-order phase derivative dynamics in a better way and the delay highlighted by Fig. 1 is dramatically reduced; zero crossing points of the estimated ROCOF are now delayed by about 4 ms instead of 25 ms. Maximum |RFE| is lowered by more than 62 %, since it drops from 23.2 to 8.7 Hz/s. These residual errors are due to the employment of an intrinsically approximated model in order to filter the estimations obtained from uncertain and noisy measurement data.

[1]From here on a 1-s subinterval is used in the graphs to better show the signals, while the maximum errors are computed on a duration of 20 s.

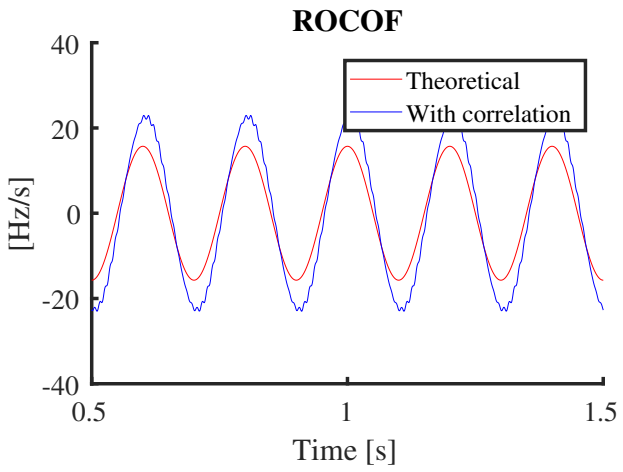

Fig. 2. ROCOF results for PM test.

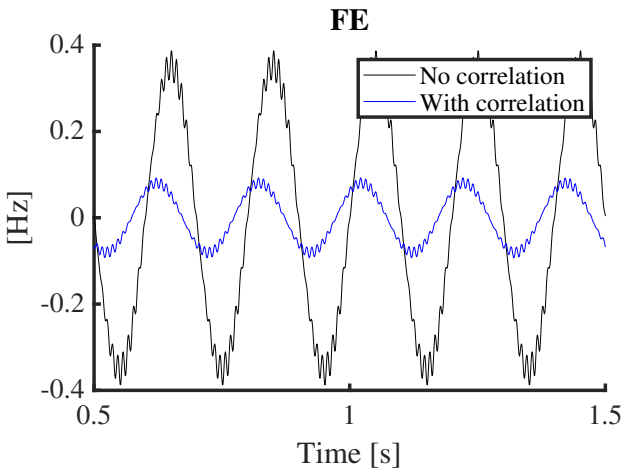

Fig. 4. FE results for PM test.

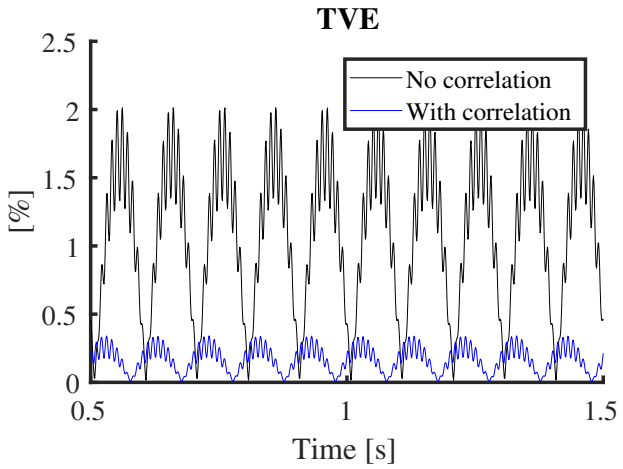

Fig. 3. TVE results for PM test.

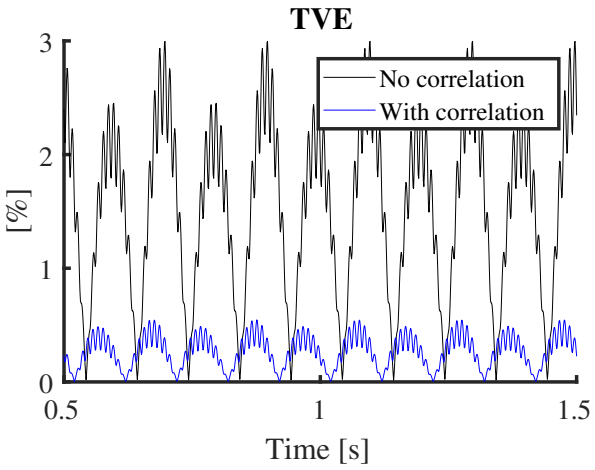

Fig. 5. TVE results for AM test.

The advantages brought by the new representation of model uncertainty are also evident in the estimates of synchrophasor and frequency. Figures 3 and 4 show the TVE and FE for the PM test, respectively, and highlight the error reduction achievable thanks to the improved tracking performance of the TEKF-corr algorithm. TVE is below $0.36\,\%$, while FE is within ± 100 mHz, hence far smaller than the corresponding errors achieved by the conventional TEKF.

Considering AM tests, similar conclusions can be drawn, even though amplitude dynamics are now involved and a different expansion order has been chosen. Fig. 5 shows the TVE for both the conventional and enhanched algorithms with 5 Hz modulation frequency and $k_x = 0.1$. The advantages in terms of error reduction are clear also in this case, since TVE reduces by $80\,\%$ thanks to the proposed approach. Table I shows the maximum values of |FE| and |RFE| in the same scenario. The errors are smaller than in the PM test case, as expected, since modulation involves only the synchrophasor amplitude, but the advantages of TEKF-corr algorithm are once again confirmed.

Finally, test waveforms containing AM and PM simultaneously (AM+PM) have been considered. Results with 5 Hz modulation frequency and $k_x = k_a = 0.1$ have been summarized in Table II. Even in this case, the accuracy improvement that can be achieved with the proposed method is evident.

TABLE I
FREQUENCY AND ROCOF ESTIMATION ERRORS FOR AM TEST.

Error Index	Without corr.	With corr.	Reduction
Max |FE| [mHz]	51.6	22.2	56.9 %
Max |RFE| [Hz/s]	1.88	1.28	31.9 %

TABLE II
SYNCHROPHASOR, FREQUENCY AND ROCOF ESTIMATION ERRORS FOR AM+PM TEST.

Error Index	Without corr.	With corr.	Reduction
Max TVE [%]	3.23	0.56	82.7 %
Max |FE| [mHz]	401	100	75.1 %
Max |RFE| [Hz/s]	23.7	8.8	62.9 %

B. Off-Nominal Frequency and Harmonic Tests

Once the improvements under dynamic test conditions have been assessed, it is important to verify that the proposed modification at the TEKF do not degrade performance under steady-state conditions. For this reason, different input signals with constant, off-nominal frequencies have been applied. Frequencies $f_1 = 45$ and $55\,\text{Hz}$ are here used to stress the filter capability to reach states which are far from the nominal ones. It can be noticed that, after the initial transient is settled, TVE, |FE| and |RFE| reach negligible values (about $10^{-10}\,\%$, $10^{-11}\,\text{Hz/s}$, and $10^{-9}\,\text{Hz/s}$, respectively). Therefore, the new uncertainty model does not significantly affect the steady-state behaviour of the estimator.

Steady-state tests have also been performed in the presence of harmonics, with different combinations of harmonic phase angles. As expected, since harmonics have been included as state variables, the synchrophasor, frequency and ROCOF estimation errors are negligible, thus establishing that TEKF-corr maintains the same harmonic rejection properties of the conventional implementation.

C. Step Change Tests

Finally, it is important to check the behaviour of the algorithm in the presence of abrupt variations such as step changes. As discussed in Section IV, the application of the proposed uncertainty description relies on the continuous check (exploiting the estimated covariances) of the compatibility between forecasted values and actual measurements.

Fig. 6 shows the TVE results for a -10° phase step, which is the most challenging step prescribed by [3]. The variation occurs at $t = 10\,\text{s}$, and the algorithms need some time to recover from the transient towards steady-state conditions. With the rules defined in Section IV, the TEKF-corr promptly detects the variation and model uncertainty is reinitialized. Thus, even if the peak TVE is high (the y-axis in the figure is limited to $10\,\%$ for a better visualization, but the maximum is about $17\,\%$), it settles in a few tens of milliseconds (e.g. in $16\,\text{ms}$ the TVE returns below $1\,\%$). Its faster response with respect to the conventional TEKF is immediately clear.

A similar behaviour can be found also for FE and RFE. Fig. 7 compares the ROCOF estimation obtained with the conventional TEKF algortithm and with the enhanced version TEKF-corr. The graph proves the importance of the proposed technique, which allows managing the model uncertainty when it is no longer adequate, thus avoiding a slower transition towards the new steady-state conditions.

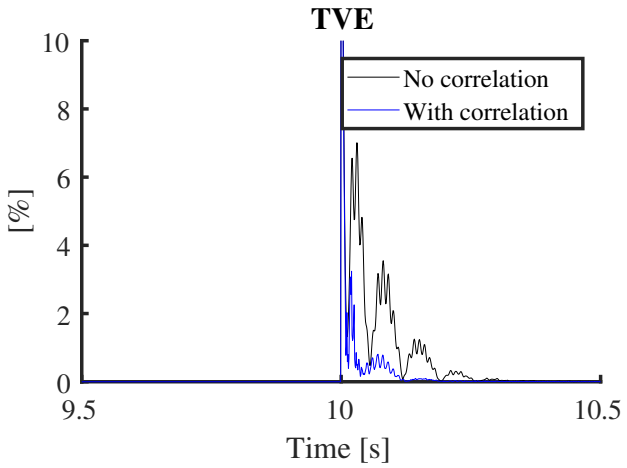

Fig. 6. TVE results for phase angle -10° step test.

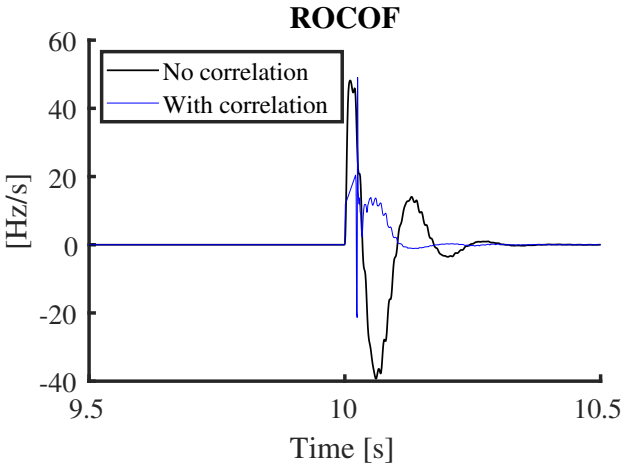

Fig. 7. RFE results for phase angle -10° step test.

VI. Conclusions

A Taylor-based Extended Kalman filter, which considers model error correlations due to signal dynamics appearing on the sampling-time scale, has been proposed as a low-latency technique for estimating synchrophasor, frequency and ROCOF. The advantages of properly modeling this phenomenon have been shown, along with a solution to deal with abrupt variations of the input signal. The comparison of measurement and forecast uncertainties is the key to detect changes and choose the most appropriate description of model uncertainty according to the actual conditions. The presented technique allows a trade-off between different situations, so that phasor, frequency and ROCOF dynamics can be tracked, while maintaining high accuracy under stedy-state conditions and properly reacting to unexpected events. Conversely to other Kalman-based solutions, model error description does not require a fine-tuning, while the proposed filter equations can be implemented without a significant computational overhead.

References

[1] AA. VV., *Phasor Measurement Units and Wide Area Monitoring Systems*, 1st ed., A. Monti, C. Muscas, and F. Ponci, Eds. Academic Press, 2016.

[2] A. G. Phadke and J. S. Thorp, *Synchronized Phasor Measurements and Their Applications*. Springer Science, 2008.

[3] *IEEE/IEC International Standard - Measuring relays and protection equipment - Part 118-1: Synchrophasor for power systems - Measurements*, IEEE/IEC IEC/IEEE 60255-118-1:2018, Dec 2018.

[4] *IEEE Standard for Synchrophasor Measurements for Power Systems*, IEEE IEEE Std C37.118.1-2011 (Revision of IEEE Std C37.118-2005), Dec. 2011.

[5] *IEEE Standard for Synchrophasor Measurements for Power Systems – Amendment 1: Modification of Selected Performance Requirements*, IEEE IEEE Std C37.118.1a-2014 (Amendment to IEEE Std C37.118.1-2011), Apr. 2014.

[6] J. A. de la O Serna, "Dynamic phasor estimates for power system oscillations," *IEEE Trans. Instrum. Meas.*, vol. 56, no. 5, pp. 1648–1657, Oct. 2007.

[7] W. Premerlani, B. Kasztenny, and M. Adamiak, "Development and implementation of a synchrophasor estimator capable of measurements under dynamic conditions," *IEEE Trans. Power Del.*, vol. 23, no. 1, pp. 109–123, Jan. 2008.

[8] R. K. Mai, Z. Y. He, L. Fu, B. Kirby, and Z. Q. Bo, "A dynamic synchrophasor estimation algorithm for online application," *IEEE Trans. Power Del.*, vol. 25, no. 2, pp. 570–578, Apr. 2010.

[9] P. Castello, J. Liu, C. Muscas, P. A. Pegoraro, F. Ponci, and A. Monti, "A fast and accurate PMU algorithm for P+M class measurement of synchrophasor and frequency," *IEEE Trans. Instrum. Meas.*, vol. 63, no. 12, pp. 2837–2845, Dec. 2014.

[10] M. A. Platas-Garza and J. A. de la O Serna, "Dynamic harmonic analysis through taylor-fourier transform," *IEEE Trans. Instrum. Meas.*, vol. 60, no. 3, pp. 804–813, Mar. 2011.

[11] M. Bertocco, G. Frigo, C. Narduzzi, C. Muscas, and P. A. Pegoraro, "Compressive sensing of a taylor-fourier multifrequency model for synchrophasor estimation," *IEEE Transactions on Instrumentation and Measurement*, vol. 64, no. 12, pp. 3274–3283, Dec 2015.

[12] S. Toscani and C. Muscas, "A space vector based approach for synchrophasor measurement," in *Instrum. and Meas. Technol. Conf. (I2MTC) Proc., 2014 IEEE Int.*, May 2014, pp. 257–261.

[13] P. Castello, R. Ferrero, P. A. Pegoraro, and S. Toscani, "Space vector taylor-fourier models for synchrophasor, frequency, and rocof measurements in three-phase systems," *IEEE Transactions on Instrumentation and Measurement*, vol. 68, no. 5, pp. 1313–1321, May 2019.

[14] I. Kamwa, S. R. Samantaray, and G. Joos, "Wide frequency range adaptive phasor and frequency pmu algorithms," *IEEE Trans. Smart Grid*, vol. 5, no. 2, pp. 569–579, Mar. 2014.

[15] J. A. de la O Serna and J. Rodriguez-Maldonado, "Instantaneous oscillating phasor estimates with taylor-kalman filters," *IEEE Trans. Power Syst.*, vol. 26, no. 4, pp. 2336–2344, Nov. 2011.

[16] J. Liu, F. Ni, J. Tang, F. Ponci, and A. Monti, "A modified Taylor-Kalman filter for instantaneous dynamic phasor estimation," in *IEEE PES Innovative Smart Grid Technologies (ISGT) Eur. Conf.*, 2012.

[17] D. Fontanelli, D. Macii, and D. Petri, "Dynamic synchrophasor estimation using smoothed kalman filtering," in *Instrum. and Meas. Technol. Conf. (I2MTC) Proc., 2016 IEEE Int.*, Taipei, Taiwan, May 2016.

[18] J. de la O Serna and J. Rodriandguez-Maldonado, "Taylor-Kalman-Fourier filters for instantaneous oscillating phasor and harmonic estimates," *IEEE Trans. Instrum. Meas.*, vol. 61, no. 4, pp. 941–951, Apr. 2012.

[19] J. Liu, F. Ni, P. A. Pegoraro, F. Ponci, A. Monti, and C. Muscas, "Fundamental and harmonic synchrophasors estimation using modified taylor-kaiman filter," in *Applied Measurements for Power Systems (AMPS), 2012 IEEE Int. Workshop on*, Sep. 2012, pp. 1–6.

[20] R. Ferrero, P. A. Pegoraro, and S. Toscani, "Dynamic fundamental and harmonic synchrophasor estimation by extended kalman filter," in *2016 IEEE International Workshop on Applied Measurements for Power Systems (AMPS)*, Sep. 2016, pp. 1–6.

[21] G. Frigo, A. Derviškadić, Y. Zuo, and M. Paolone, "PMU-based rocof measurements: Uncertainty limits and metrological significance in power system applications," *IEEE Transactions on Instrumentation and Measurement*, vol. 68, no. 10, pp. 3810–3822, Oct. 2019.

Roberto Ferrero (S'10-M'14-SM'18) received his PhD degree (cum laude) in Electrical Engineering from Polytechnic of Milan, Italy, in 2013. He has been a lecturer with the Department of Electrical Engineering and Electronics, University of Liverpool, UK, since 2015. His main research activity is focused on electrical measurements, particularly applied to power systems and electrochemical devices. He is a member of the IEEE Instrumentation and Measurement Society, and of its TC 39 (Measurements in Power Systems). He has been an Associate Editor of the IEEE Transactions on Instrumentation and Measurement since 2017.

Paolo Attilio Pegoraro (M'06-SM'19) received the M.S. (summa cum laude) degree in telecommunications engineering and the Ph.D. degree in electronic and telecommunications engineering from the University of Padova, Padua, Italy, in 2001 and 2005, respectively. From 2015 to 2018 he was an Assistant Professor with the Department of Electrical and Electronic Engineering, University of Cagliari, Cagliari, Italy, where he is currently Associate Professor. He has authored or co-authored over 90 scientific papers. His current research interests include the development of new measurement techniques for modern power networks, with attention to synchronized measurements and state estimation. Dr. Pegoraro is a member of IEEE Instrumentation and Measurement Society TC 39 (Measurements in Power Systems) and of IEC TC 38 (Instrument Transformers). He is an Associate Editor of the IEEE Transactions on Instrumentation and Measurement.

Sergio Toscani (S'08, M'12, SM'19) received the M.Sc. (cum laude) and the Ph.D degree in electrical engineering from the Politecnico di Milano, Milan, Italy, in 2007 and 2011 respectively. Since 2011 he is Assistant Professor in Electrical and Electronic Measurement with the Dipartimento di Elettronica, Informazione e Bioingegneria of the same University. His research activity is mainly focused on development and testing of current and voltage transducers, measurement techniques for powers systems, electrical components and systems diagnostics. Dr. Sergio Toscani is member of the IEEE Instrumentation and Measurement Society and of the TC-39 - Measurements in Power Systems.